Electronic Supplementary Material (ESI) for Journal of Materials Chemistry A

Electronic Supplementary Information

High electrocatalytic activity of low-loaded transparent carbon nanotube assemblies for $Co^{II/III}$-mediated dye-sensitized solar cells

Seon Hee Seo,[*a] Mi Hyung Kim,[a] Eun Ji Jeong,[ab] Sung Hwan Yoon,[a] Hyon Chol Kang,[b] Seung I. Cha[a] and Dong Yoon Lee[a]

[a]Nano Hybrid Technology Research Center, Korea Electrotechnology Research Institute, Changwon 641-120, Korea.

[b]Department of Advanced Materials Engineering, College of Engineering, Chosun University, Gwangju 501-759, Korea.

*Corresponding author: seosh@keri.re.kr

1. Experimental Details

Fabrication of TiO_2 photo-anodes

To fabricate the photo-anodes for the DSCs, compact TiO_2 layers were introduced on bare FTO glasses from a solution of diisopropoxytitanium bis(acetylacetonate) in isopropanol (Aldrich) by screen printing. The formed layers were then heated at 500 °C for 15 min. To form mesoporous TiO_2 layers, 5 g of anatase TiO_2 nanoparticles (particle size <25 nm, 99.7%, Aldrich) were mixed with 0.5 g of dodecanoic acid (Fluka) in 150 ml of anhydrous ethanol and ball-milled for 3 days. 2.2 g of the resultant dried powder was mixed with 10 g of ethanol solution containing 10 wt% ethyl cellulose (EC, viscosity 46 cP, 5 % in toluene/ethanol 80:20, Aldrich) and 10 g of α-terpineol (90%, Aldrich). After ball-milling of the mixture, the remaining ethanol was evaporated. The resultant viscous paste was milled in a three-roll mill, which gives a 3.7-μm-thick transparent TiO_2 layer per a screen printing (200 mesh, stainless steel). In order to enhance the photocurrent of the normal DSCs, a 7-μm-thick scattering layer (PST-400C, CCIC-JGC, Japan) was prepared on top of the dried transparent layer. In case of the transparent bifacial DSCs, the top layer was replaced with a 1.4-μm-thick highly transparent TiO_2 layer prepared by modifying a commercial TiO_2 paste (PST-18NR, CCIC-JGC, Japan). 6 g of PST-18NR was mixed with 11.6 g of 10 wt% EC ethanol and 6 g of terpineol and the rest processes were similar to those for the bottom transparent TiO_2 layer. After the annealing of the TiO_2 layers at 480 °C for 60 min, the TiO_2 electrodes were immersed in a 30 mM aqueous solution of TiCl4 for 30 min in an oven at 70 °C and then washed with water. Finally, the TiCl4-treated TiO_2 electrodes were annealed at 450 °C for 30 min, and then soaked in 0.3 mM toluene solution of the dye MK-2 (2-Cyano-3-[5‴-(9-ethyl-9H-carbazol-3-yl)-3′,3″,3‴,4-tetra-n-hexyl-[2,2′,5′,2″,5″,2‴]-quaterthiophen-5-yl] acrylic acid, Aldrich) dye at RT for 15 h.

Calculation of the electroactive surface area

The electroactive surface area for the reduction of the electroactive species can be estimated from cathodic peak current ($I_{p,c}$) using the Randles-Sevcik equation: [S1]

$$I_{p,c} = (2.69 \times 10^5) n^{3/2} A D^{1/2} C \nu^{1/2}$$

where n is the number of electrons exchanged, A is the electroactive surface area, D is the diffusion coefficient, C is the concentration of the electroactive species, and ν is the scan rate. For the $Co(bpy)_3^{2+/3+}$ redox reaction, using n = 1, D = 6.4 × 10^{-6} cm^2/s, and the values of $I_{p,c}$ measured on the basis of the capacitive backgrounds, the electroactive surface areas of the ca-SWNT electrodes assembled on hydroxyl and APTES-modified FTO substrates were estimated at 0.348 cm^2 and 0.361 cm^2, respectively, for the reduction of the $Co(bpy)_3^{3+}$ redox mediator.

Calculation of the charge-transfer resistance (R_{CT})

The EIS data obtained using the symmetrical closed dummy cells were interpreted using the well-known equivalent electrical circuit shown in Scheme S2.[S2] EIS involves the charge-transfer impedance at the electrode/electrolyte interface (Z_{CT}) in the high-frequency region and the diffusion impedance (Z_D) of the electroactive species within the electrolyte in the low-frequency region. The x intercept of the high-frequency domain is associated with the frequency-independent ohmic resistance (R_0).

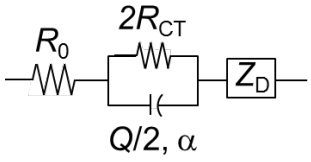

To obtain a better fit, rather than using capacitance, we adopted a constant phase element (CPE) with an exponent α. The deviation of α from 1 represents the reactivity distribution of the electrode. When α = 1, the CPE behaves as a capacitor and R_{CT} is equal to the radii of the semicircles measured using the symmetrical closed dummy cells. The effective double-layer capacitance (C_{dl}) was also estimated from Q, α, and ω_{max} on the basis of the following relationship, $C_{dl} = Q(\omega_{max})^{\alpha-1}$, where ω_{max} is the peak frequency at which the imaginary part of the impedance reaches its maximum.[S2]

Calculation of the diffusion coefficient of $Co(bpy)_3^{3+}$

The limiting current density (J_{lim}) (A/cm^2) depends on the diffusion of the electroactive species in the thin-layer cell and can be approximated using Fick's first law as follows:

$$J_{\lim} = 2nFD_O \frac{C_O}{d}$$

where D_O is the diffusion coefficient of the reduced form of redox couples (cm^2/s), d is the spacer thickness (cm), C_O is the concentration (mol/cm^3), F is the Faraday constant, and n is the number of electrons involved in the electrode reaction. For the $Co(bpy)_3^{2+/3+}$ redox reaction in a thin-layer cell, we used n=1, C_O=45 mM, and d=23 μm.

2. Supplementary data

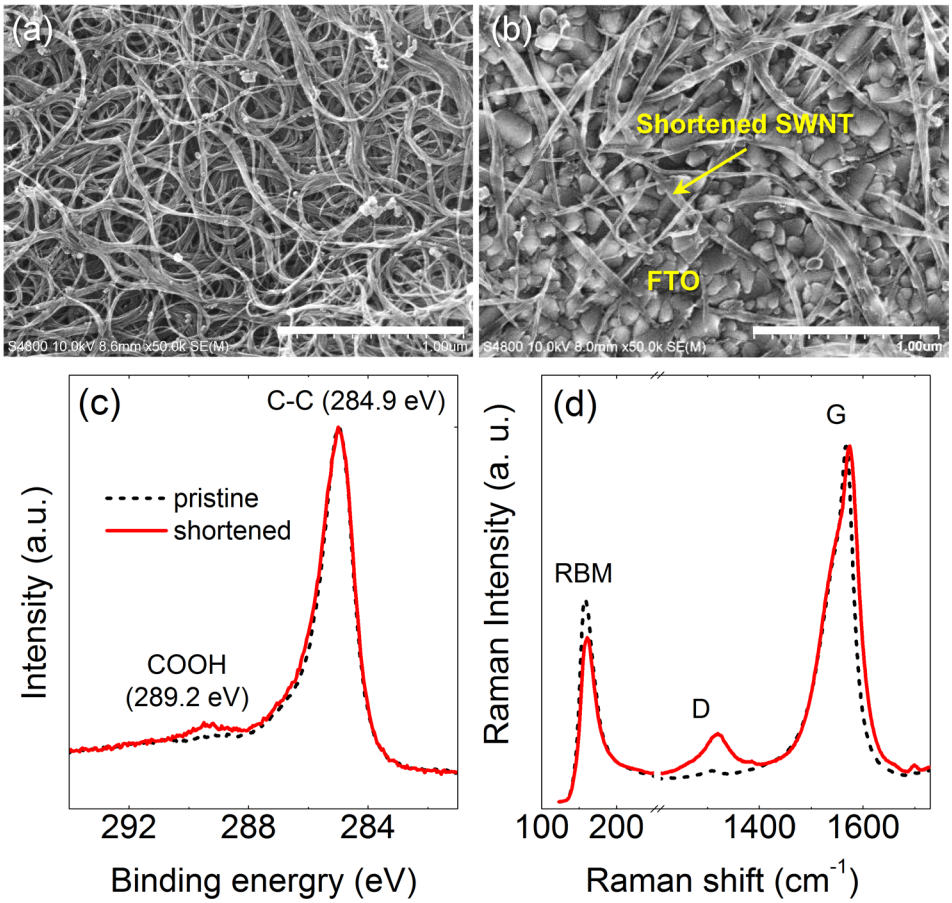

Fig. S1 SEM images for (a) the pristine SWNT powder and (b) the spray-coated shortened SWNTs, functionalized for 10 h in an acid solution, on a FTO glass. Scale bars are 1 μm. (c) XPS and (d) Raman spectra confirmed that the shortened SWNTs were mainly functionalized with carboxyl groups.

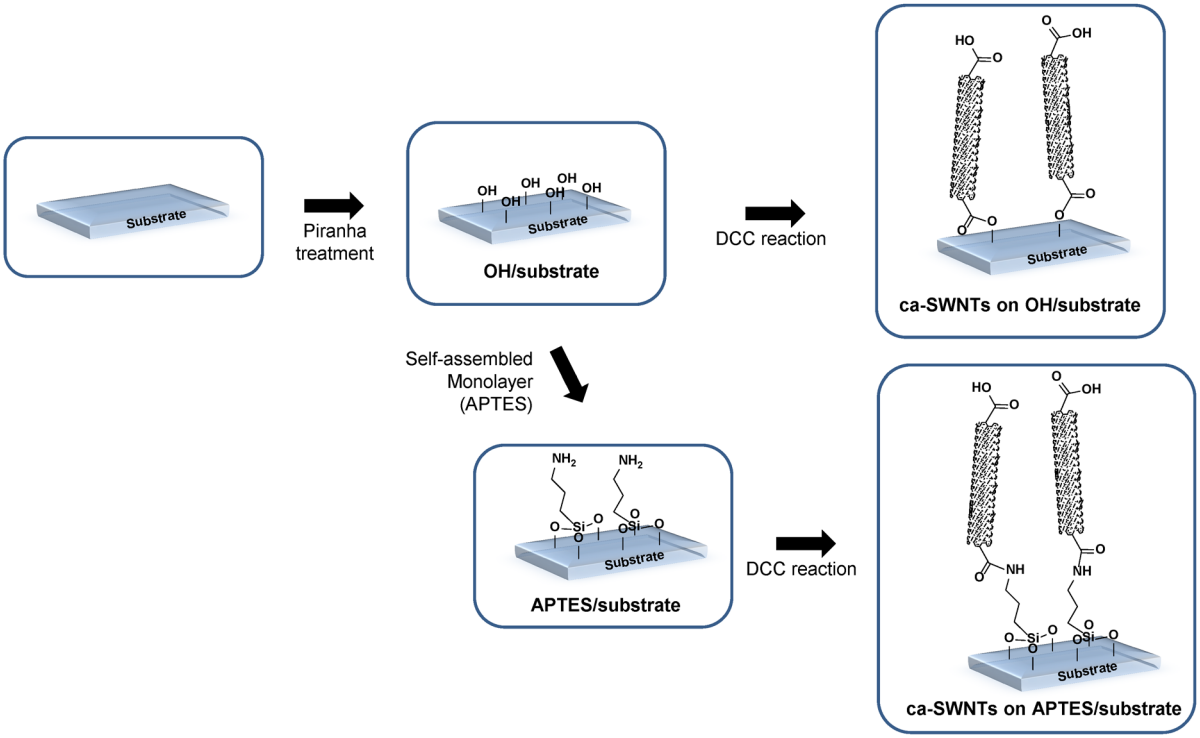

Fig. S2 A schematic illustration of the fabrication procedure of the ca-SWNT electrodes.

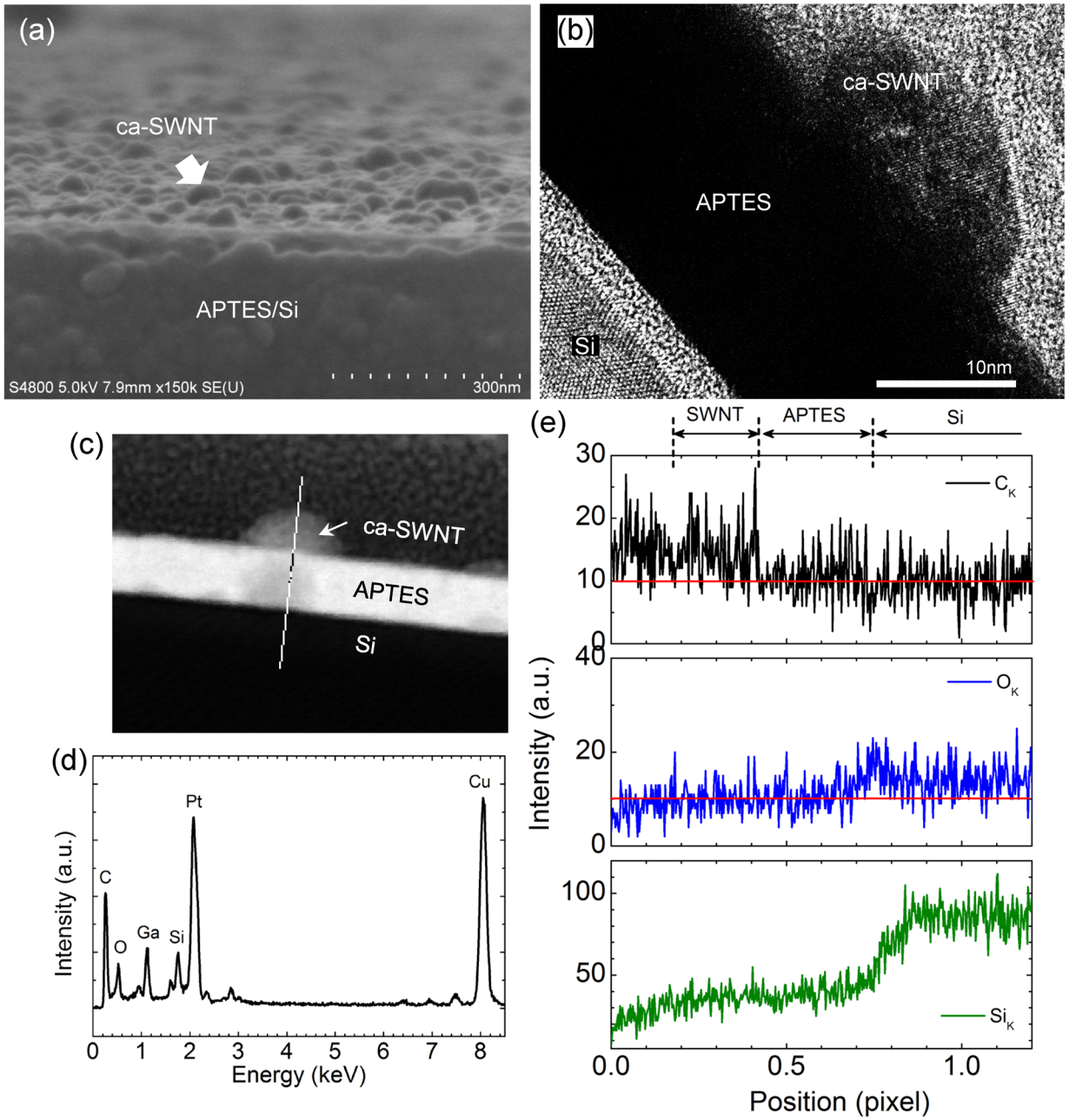

Fig. S3 Cross-sectional (a) SEM and (b) TEM images of ca-SWNTs on APTES/Si substrates after the DCC reaction for 21 h. A SEM image showed the ca-SWNTs were of wide distribution in their sizes. A TEM image presented well-defined, densely packed lattice structure in a ca-SWNT domain. To confirm the elemental distribution, we undertook the energy dispersive x-ray (EDX) analysis during a TEM measurement. (c) A scan of the selected area in a TEM image. (d) An EDX profile measured from the region in Fig. S3c. It is noteworthy that Ga and Pt signals originated from Ga atoms implanted during a focused ion beam process and a capping layer, respectively. A Cu signal originated from the TEM grid. (e) Intensity profiles of characteristic emissions for C_K, O_K, and Si_K, measured across the sample

indicated by the white arrow in Fig. S3c. C_K signals from the SWNT are shown clearly, while no noticeable O_K signals in the SWNT area. This indicates that the ca-SWNT composed of purely carbon rather than impurities during the DCC reaction. Red horizontal lines representing the background level are guides for eyes.

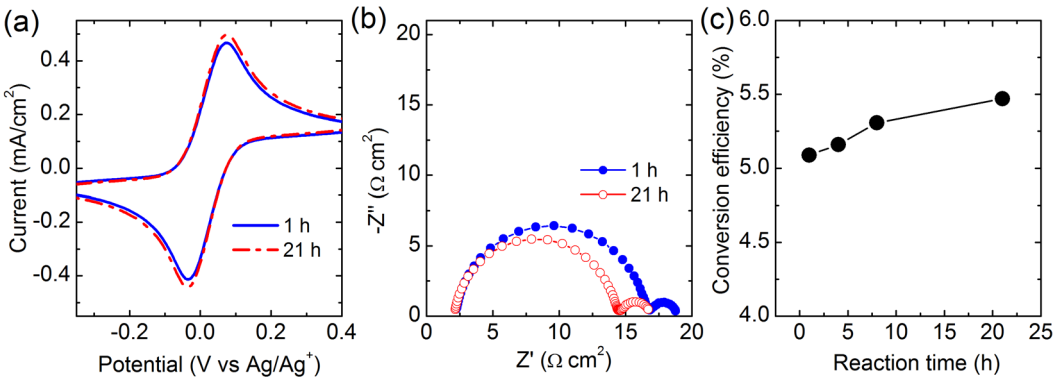

Fig. S4 (a) CVs for 2 mM $[Co(bpy)_3](PF_6)_2$/0.1 M TBA·PF_6 in acetonitrile using a three-electrode configuration. The ca-SWNT electrodes used were formed for DCC reaction time of 1 h and 21 h. (b) The Nyquist plot of the EIS data obtained under an open-circuit condition using symmetrical closed dummy cells consisting of two identical electrodes. The geometrical configuration and the electrolyte used were the same as those in the DSCs. R_{CT} was estimated by fitting the EIS data using symmetrical dummy cells on the basis of a well-established equivalent circuit[S3] (see Experimental Details of ESI). R_{CT} roughly corresponds to the radius of a semicircle at a higher frequency in the Nyquist plot. (c) Power conversion efficiencies of DSCs fabricated with the ca-SWNT CEs assembled for different reaction times.

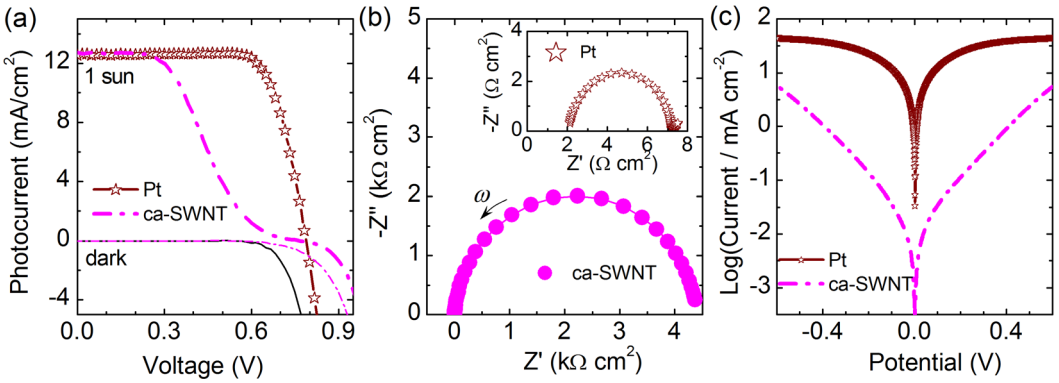

Fig. S5 (a) Photovoltaic and (b, c) electrochemical characterizations for I^-/I_3^- redox electrolyte employed in DSCs and symmetrical dummy cells with the ca-SWNT or Pt counter electrodes. The iodine-based DSCs employed a conventional double-layer (14 + 6 μm) TiO_2 photo-anode sensitized with ruthenium-based N719 dye described in elsewhere.[S4] The I^-/I_3^- -based electrolyte consisted of 0.8 M 1,2-dimethyl-3-propylimidazolium iodide (DMPImI), 0.05 M LiI, 0.1 M I_2, 0.1 M guanidine thiocyanate (GuNCS), and 0.5 M 4-*tert*-butylpyridine (tBP) in acetonitrile.

Table S1. Photovoltaic parameters of iodine-based DSCs under the illumination of 100 mW/cm^2 (1 sun) and interfacial R_{CT} of symmetrical closed dummy cells at an open-circuit voltage.

CE	V_{OC} (V)	J_{SC} (mA/cm^2)	FF	η (%)	R_{CT} (Ω cm^2)
Pt	0.788	12.56	0.751	7.43	2.6
ca-SWNT	0.767	12.69	0.383	3.73	2,194

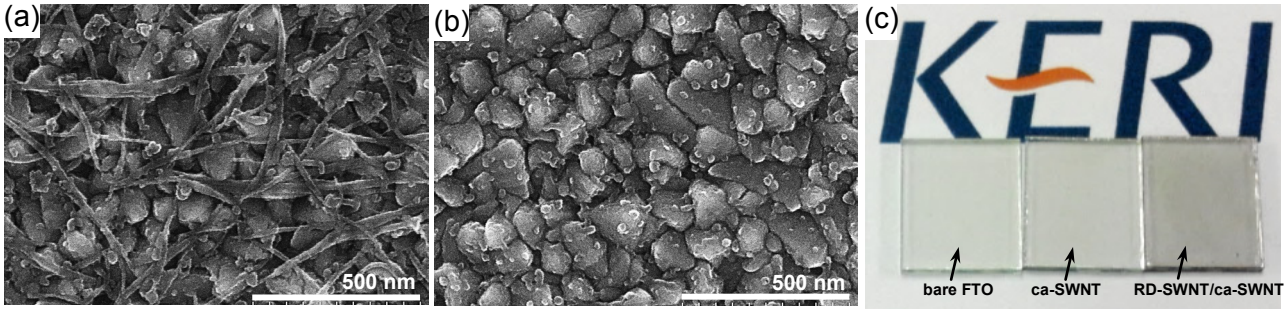

Fig. S6 Top-view SEM images of an SWNT assembly (a) before and (b) after it was washed ultrasonically in acetone for 60 s. The unwashed SWNT assembly incorporated randomly-distributed SWNTs (RD-SWNTs) on top of the ca-SWNTs. (c) A photograph of the various SWNT assemblies on FTO glasses.

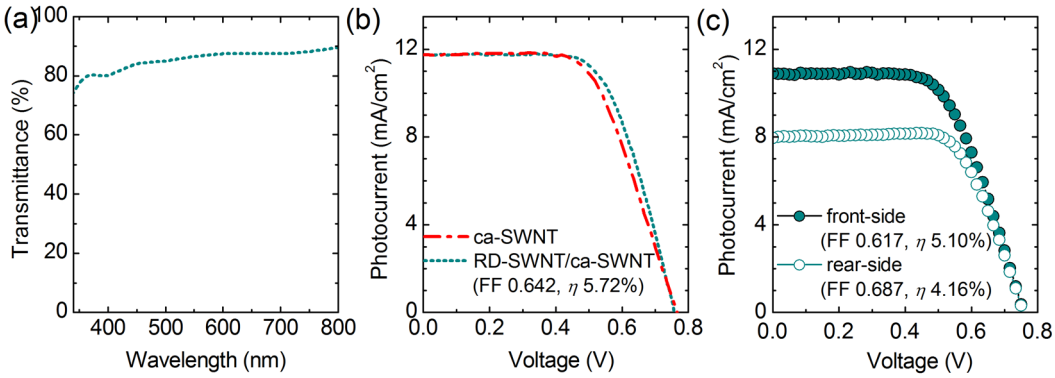

Fig. S7 (a) Transmittance of the RD-SWNT/ca-SWNT on the basis of FTO glass. (b, c) Photovoltaic *J–V* curves of DSCs with the RD-SWNT/ca-SWNT CE. The dye-sensitized TiO_2 photo-anode consisted of a transparent and an opaque layer in the case of the normal opaque DSCs (b) and only a transparent layer in the case of the semi-transparent bifacial DSCs (c).

In this work, the wet assembly method used could increase the electroactive surface area only to a limited degree. As a result, we tried to use the unwashed RD-SWNTs physically adsorbed onto the ca-SWNTs (RD-SWNT/ca-SWNT) after the chemical assembly process. The physically adsorbed SWNTs were a few micrometres in length (Fig. S6) and supported a slightly higher FF of 0.642 and η of ~5.72%. However, the transmittance of the RD-SWNT/ca-SWNT electrode decreased substantially to 85.7% (Fig. S7a). We used both the ca-SWNT and the RD-SWNT/ca-SWNT CEs in bifacial DSCs to demonstrate the high performance of transparent CEs.

References

S1 Bard, A. J.; Faulkner, L. R. *Electrochemical Methods: Fundamentals and Applications*, 2nd ed., Wiley, New York, **2000**, pp. 231–239.

S2 M. E. Orazem and B. Tribollet, *Electrochemical Impedance Spectroscopy*, Wiley, New Jersey, 2008, Chapter 13.

S3 A. Hauch and A. Georg, *Electrochim. Acta*, 2001, **46**, 3457–3466.

S4 S. H. Seo, S. Y. Kim, B.-K. Koo, S.-I. Cha and D. Y. Lee, *Langmuir*, 2010, **26**, 10341–10346.